THE JOURNAL OF PHYSICAL CHEMISTRY LETTERS
A JOURNAL OF THE AMERICAN CHEMICAL SOCIETY

pubs.acs.org/JPCL
Letter

Nonlinear Optical Spectroscopy of Molecular Assemblies: What Is Gained and Lost in Action Detection?

Luca Bolzonello, Matteo Bruschi, Barbara Fresch, and Niek F. van Hulst*

Cite This: *J. Phys. Chem. Lett.* 2023, 14, 11438−11446
Read Online

ABSTRACT: This study elucidates the information content that is extracted from action-2D electronic spectroscopy (A-2DES) when the output intensity is not proportional to the number of excitations generated. Such a scenario can be realized in both fluorescence and photocurrent detection because of *direct* interaction like exciton−exciton annihilation or *indirect* effects in the signal generation or detection. By means of an intuitive probabilistic model supported by nonlinear response theory, the study concludes that in molecular assemblies the ground-state bleaching contribution can dominate the nonlinear signal and partially or completely hide the stimulated emission. In this case, the spectral effect resembles incoherent mixing, even in the absence of exciton−exciton annihilation, implying reduced information about the excited-state dynamics with an increasing number of chromophores. This finding has important implications for the selection of samples for A-2DES as well as for its interpretation.

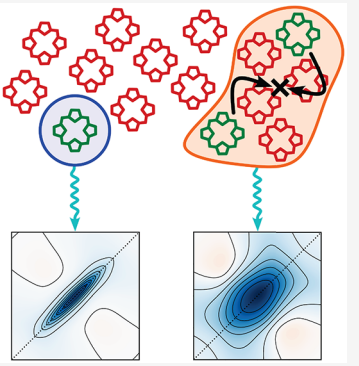

Action-2D electronic spectroscopy (A-2DES) has been attracting significant attention due to its advantages compared to conventional coherent-2D electronic spectroscopy (C-2DES). Both techniques are employed to investigate the dynamics of complex multichromophoric systems. In C-2DES, the observable is a *coherent* electric field originating from the macroscopic polarization of the sample induced by a sequence of laser pulses.[1,2] Conversely, in A-2DES, the observable is an *incoherent* signal proportional to the excited-state population generated by the light−matter interaction.[3,4] The nature of this incoherent observable connects 2DES to almost any kind of signal, i.e., fluorescence,[5] photocurrent,[6−8] photoions,[9] and photoelectrons,[10,11] allowing for the study of a wide range of systems under *operando* conditions.[12] Furthermore, A-2DES can be combined with microscopy techniques[13] or even single-molecule detection.[14] However, the difference between the information obtained from the two techniques is a matter of debate. Indeed, the third-order polarization detected in C-2DES cannot be simply reconstructed from the fourth-order population generated in A-2DES. Indeed, while in C-2DES, the signal is emitted over an ultrafast time scale (ps) limited by the dephasing of the optical coherence, in A-2DES, the incoherent signal is collected over a longer time scale (>ns) during which the excited-state population may undergo several processes during the detection.

Among these processes, we recognize the internal conversion from excited states with higher energy to the lowest one, from which fluorescence occurs according to Kasha's rule.[15] Another example is represented by exciton−exciton annihilation (EEA) in multichromophoric systems[5,13,16] and Auger recombination in nanostructures,[7,17,18] both resulting in the net loss of an exciton. These processes underlie the emergence of cross-peaks in the spectrum at early waiting times.[19−21] Furthermore, it has been reported how the phenomenon of incoherent mixing can affect A-2DES spectra.[22] In this case, due to nonlinear population dynamics,[22] e.g., exciton−exciton annihilation and Auger recombination, or to nonlinearities in the detection process,[23] linear responses can mix during the detection entering the signal and potentially masking the nonlinear response of the system.[22,24,25]

The equivalence between the origin of cross-peaks at early waiting times and the phenomenon of incoherent mixing was recently demonstrated for a weakly interacting molecular dimer in the presence of EEA.[25] However, it is not yet clear how incoherent mixing affects the response in the case of multichromophoric systems and whether other mechanisms beyond EEA may lead to the same spectral features. This paper clarifies these aspects. Specifically, we will show that in the case of molecular assemblies, (i) cross-peaks related to incoherent mixing translate into the dominance of the ground-state bleaching over the stimulated emission contribution of the signal and (ii) the effect does not necessarily require *direct* interaction between excitons, e.g., EEA or Auger recombination, but it can result from other *indirect* interactions. To give a concrete example, natural photosynthetic proteins, such as

Received: October 10, 2023
Revised: November 22, 2023
Accepted: December 5, 2023
Published: December 12, 2023

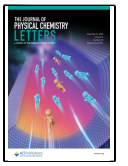

https://doi.org/10.1021/acs.jpclett.3c02824
J. Phys. Chem. Lett. 2023, 14, 11438−11446

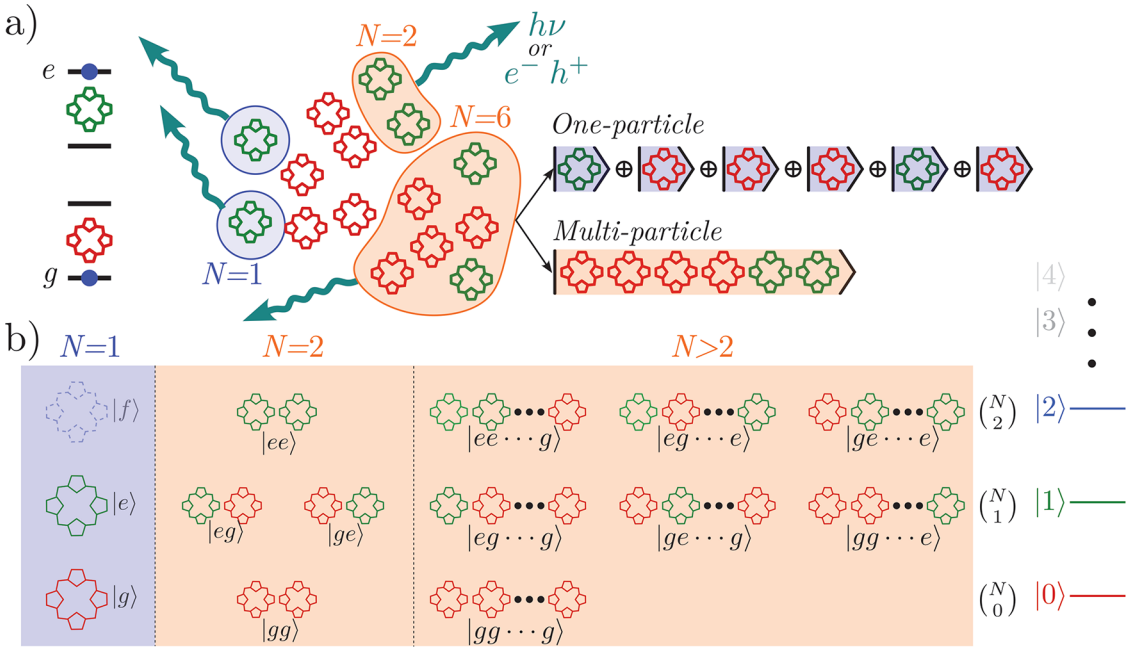

Figure 1. In action spectroscopy, the detected signal is proportional to the excited-state population. (a) In an ensemble of identical molecules, represented as two-level systems, the signal is proportional to the number of excited molecules. The molecules can be independent (blue-circled) or grouped in assemblies of N molecules (orange-circled) emitting a single output. The state of the assembly can be represented using a single-particle or a multiparticle description. (b) From the multiparticle perspective, the states can be distinguished into different manifolds $|k\rangle$, depending on the number of excitons k. The number of states in each manifold is determined by the binomial coefficient $\binom{N}{k}$.

photosystems I and II or light harvesting complex 1 (LH1), contain a high number of chromophores but only one reaction center.[26] If two excitations are generated, they can directly interact, leading to EEA. However, if one excitation reaches the reaction center, it influences the fate of the second excitation in a very indirect way. Indeed, as long as the charge separation step is slower than the exciton lifetime, the second excitation will eventually relax to the ground state because of the impossibility of reaching the reaction center. These additional nonlinearities are characteristic of action detection schemes, implying a mismatch between action- and coherent-detected spectra.

The light−matter interaction is commonly described in the framework of response theory.[27] The nonlinear signal is given by higher-order terms in the response that allow a comprehensive explanation of the quantum dynamics of the system. At the same time, these theoretical tools could drive the spectroscopist far from a more practical and experimental approach. For this reason, here, we examine the contributions to the signal using two approaches.

The first approach involves the probabilistic description of the light−matter interaction considering an assembly of N molecules. This approach aims to identify the sources of nonlinearity in cases where the number of readable outputs differs from the number of molecules excited. In other words, we are referring to those systems where more than one exciton can be excited, such as multichromophoric systems as well as quantum dots, but a smaller number of excitons can be detected because of exciton−exciton annihilation, Auger recombination, internal conversion, or limited charge separation.

The second approach translates these findings into the framework of the response theory. The nonlinear signal is given by several contributions related to the different pathways followed by the system upon the light−matter interaction. For the third-order polarization, these contributions are ground-state bleaching (GSB), stimulated emission (SE), and excited-state absorption (ESA), commonly used to describe the signal in pump−probe spectroscopy and 2DES. As anticipated, in the context of action-detected techniques, the readout involves the detection of the fourth-order population, i.e., the number of excitons after the pulse train. If populations decay through processes other than the emission, then the signal could suffer from nonlinearities beyond the optical one. To include these, it is useful to distinguish between the nonlinear terms involving a single molecule and those involving different molecules in the same assembly. Throughout our discussion, we assume excitations with a local character and therefore weak coupling between distinct absorbing units.

Let us start by considering an assembly of N identical molecules, each described by a ground state $|g\rangle$ and an excited state $|e\rangle$ (Figure 1a). In the multiparticle basis, the state of the assembly is given by accounting for the state of each molecule simultaneously.[21,25,28] The states can be distinguished into different manifolds that differ by the number of excited molecules (Figure 1b). The number of states in each manifold $|k\rangle$ scales as the binomial coefficient:

$$\binom{N}{k} = \frac{N!}{k!(N-k)!} \tag{1}$$

where k is the number of excitons. In the following, each assembly is assumed to contribute to the signal with a single output, i.e., one photon emission or one charge separation. We stress that this simple assumption mimics indistinctly very different scenarios: the presence of nonlinear population dynamics, e.g., EEA or Auger recombination, nonlinear signal generation, e.g., charge separation in photosynthetic systems, or nonlinearities in the detection, e.g., single-photon detector.

https://doi.org/10.1021/acs.jpclett.3c02824
J. Phys. Chem. Lett. 2023, 14, 11438−11446

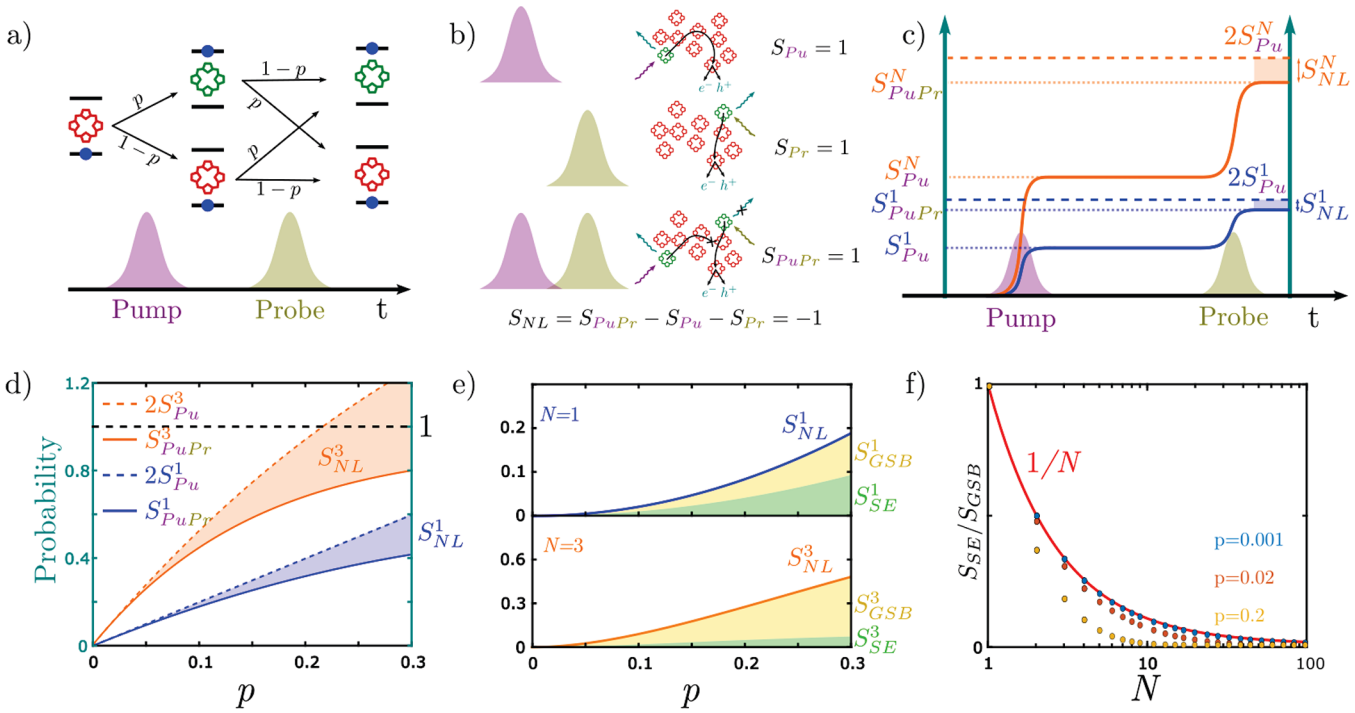

Figure 2. Simulation of action-detected pump−probe experiment for a molecular assembly. (a) An assembly interacts with two pulses, namely pump and probe. For each pulse, a molecule can either undergo a transition with probability p or remain in the same state with probability $1 - p$. (b) The nonlinear signal is given by the difference between the pump−probe signal S_{PuPr} and that of independent pump and probe S_{Pu} and S_{Pr}. The depiction of an assembly shows how part of the nonlinear signal originates from the excitation of distinct molecules by different pulses, which happens if the two excitations undergo annihilation or share the same reaction center for charge separation. (c) A schematic representation illustrating the pump−probe experiment. The interaction with the pump excites molecules in the assembly with a certain probability. By finding the assembly in a different population state, the interaction with the probe does not double the probability of molecules being in the excited state, giving rise to the nonlinear signal. (d) Signal from the pump−probe (solid line), signal from two independent pulses (dashed line) and nonlinear signal (infill area) as a function of the transition probability p for an assembly with $N = 1$ (blue) and $N = 3$ (orange). (e) Decomposition of the nonlinear signal in GSB and SE contributions for $N = 1$ and $N = 3$. (f) The ratio between SE and GSB contributions follows $1/N$ for $p \to 0$, while it decreases for higher values.

Initially, all of the molecules are in their ground state. Then, they interact subsequently with two identical laser pulses, termed the pump and probe in analogy with spectroscopy. At each pulse, a molecule can undergo an electronic transition with probability $p = I\sigma$, where I is the photon fluence and σ is its cross section, or remain in the same state with probability $1 - p$ (Figure 2a). In a realistic assembly, molecules can have different orientations; thus, p would be different for each molecule. For the sake of simplicity, we keep p equal for all molecules; however, the main conclusions hold in the more general case.

After the pump pulse, the probability of having a certain number of molecules in excited state $P_{N,k}$ follows the binomial distribution:

$$P_{N,k} = \binom{N}{k} p^k (1-p)^{N-k} \tag{2}$$

We define the probability of detecting a signal after the pump pulse as the probability of having at least one molecule excited in the assembly:

$$S^N_{\mathrm{Pu}} = 1 - P_{N,0} = 1 - (1-p)^N \tag{3}$$

where $(1 - p)^N$ represents the probability that none of the N molecules get excited. Notice that for $N = 1$, the signal simply reduces to $S^1_{\mathrm{Pu}} = p = I\sigma$, that is, the probability of exciting an independent molecule. Within the same detection setting, the signal after the pump−probe sequence is again proportional to the probability of having at least one excitation in the system. This can be evaluated from the probability of the complementary event, that is, every molecule is in the ground state. This is true if each molecule undergoes either no transition $(1 - p)^2$ or two transitions p^2:

$$S^N_{\mathrm{PuPr}} = 1 - [(1-p)^2 + p^2]^N \tag{4}$$

The nonlinear signal is obtained by subtracting the pump−probe signal from that of the independent pump and probe pulses (Figure 2c):

$$S^N_{\mathrm{NL}} = 2S^N_{\mathrm{Pu}} - S^N_{\mathrm{PuPr}} = 2[1 - (1-p)^N] - \{1 - [(1-p)^2 + p^2]^N\} \tag{5}$$

From the spectroscopic point of view, the nonlinear signal can be extracted by modulating the amplitude of the pulses using a chopper (Figure 2b), as done in two-pulse action-detected experiments.[29−32]

In Figure 2d, we report the nonlinear signal for two assemblies with different numbers of molecules, $N = 1$ and $N = 3$. We notice that for $N = 1$ the nonlinearity comes only from the double interaction with the pulses as S^1_p is linear with p, while for $N > 1$, even the signal from the single pulse is nonlinear, according to eq 3. Notice that because a single output is detected, the nonlinear signal saturates at 1 for any value of N. However, the probability of measuring an output

https://doi.org/10.1021/acs.jpclett.3c02824
J. Phys. Chem. Lett. 2023, 14, 11438−11446

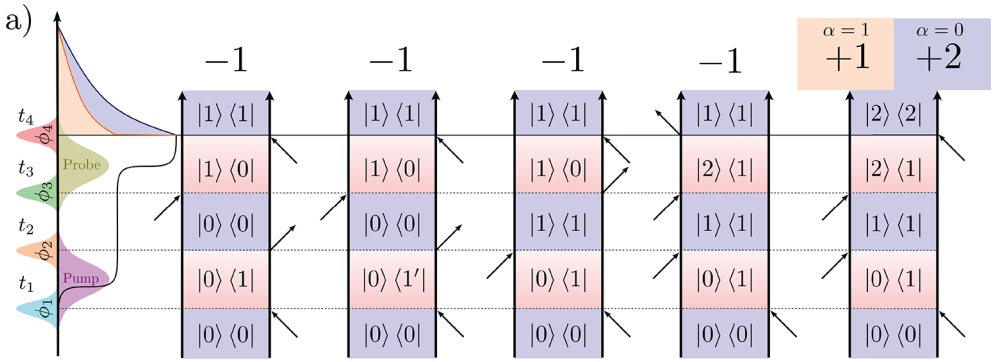

b)

α	GSB^s	GSB^c	SE^s	ESAI^c	ESAII^c
0	$-N$	$-N(N-1)$	$-N$	$-N(N-1)$	$2N(N-1)$
(0, 1)	$-N$	$-N(N-1)$	$-N$	$-N(N-1)$	$(2-\alpha)N(N-1)$
1	$-N$	$-N(N-1)$	$-N$	$-N(N-1)$	$N(N-1)$

Figure 3. (a) Feynman diagrams for ground-state bleaching (GSB), stimulated emission (SE), excited-state absorption I (ESAI), and excited-state absorption II (ESAII) of the rephasing signal in A-2DES. The diagrams are distinguished into self-population pathways "s", if the four pulses interact with the same chromophore, and cross-population pathways "c", if each pair of pulses interacts with different chromophores. (b) Table reporting the number of contributions to the signal for each kind of pathway, in the case of different values of the coefficient α. For $\alpha = 0$, there is mutual cancellation between cross-population pathways, while for $\alpha = 1$, only ESA-type pathways mutually cancel.

increases steeper as N becomes larger. Therefore, at this stage, we can already highlight two different sources of nonlinearity: the optical nonlinearity due to the interaction with the two laser pulses and the nonlinearity in the signal detection due to the measurement of a single output.

However, before aiming at these classifications, it is convenient to identify two complementary nonlinear contributions: the stimulated emission (SE) and ground-state bleaching (GSB). The SE signal is given by the process in which the probe deexcites a molecule that has been excited by the pump. Because this event is detected only when it leads to a change in the signal, if another molecule in the assembly gets excited, the double transition would result unmeasured. Thus, in our model, the SE signal is defined as the probability that at least one molecule in the assembly undergoes two transitions and the final output is vanishing:

$$S_{SE}^N = [(1-p)^2 + p^2]^N - (1-p)^{2N} \tag{6}$$

where $[(1-p)^2 + p^2]^N$ is the probability of vanishing output from the assembly, while $(1-p)^{2N}$ is the probability that all molecules undergo no transitions.

Instead, the GSB signal is given by the probability that the probe excites at least one molecule in the assembly given that the pump has already excited another molecule, as this would give no additional signal:

$$S_{GSB}^N = [1 - (1-p)^N]^2 \tag{7}$$

In other words, this is the lack of signal because the assembly has been excited by the pump. The nonlinear signal corresponds to the sum of the GSB and SE contributions:

$$S_{NL}^N \equiv S_{GSB}^N + S_{SE}^N \tag{8}$$

In Figure 2e, we show the decomposition of the nonlinear signal into SE and GSB contributions. For $N = 1$, the two contributions are equal to $S_{SE}^1 = S_{GSB}^1$ as expected for independent molecules, while for $N > 1$, S_{GSB}^N becomes larger than S_{SE}^N. As shown in Figure 2f, their ratio is

$$\frac{S_{SE}^N}{S_{GSB}^N} \leq \frac{1}{N} \tag{9}$$

where the equality holds in the limit of small transition probabilities, $p \to 0$.

The probabilistic approach can be connected to the perturbative framework of nonlinear response theory, thus enabling the analysis of action-detected 2D experiments. In four-pulse A-2DES, the components of the fourth-order signal are typically selected using phase-cycling[33,34] or phase-modulation[35] schemes. The pulses are separated by delay times t_1, t_2, and t_3, while the emission of the incoherent signal occurs during t_4. At each light−matter interaction, the state of the system changes from population to coherence, and vice versa. Therefore, each second-order interaction, which occurs with probability p in the pump−probe picture discussed above, is replaced by two first-order interactions in the four-pulse setting (Figure 3a).

Without loss of generality, we limit our analysis to the case where only one- and two-exciton manifolds, denoted as $|1\rangle$ and $|2\rangle$ in Figure 1b, are populated with a non-negligible probability at the end of the pulse train. As shown in Figure 1b, these manifolds consist of all of the states in which one or two molecules are excited. We define $P_{e_n g}$ as the probability that the system is in the collective state $|g_1 ... e_n ... g_N\rangle$ in the one-exciton manifold and $P_{e_n e_m}$ as the probability of being in the state $|g_1 ... e_n ... e_m ... g_N\rangle$ in the two-exciton manifold.

In experiments, the incoherent signal is typically integrated along the detection time t_4. The time-integrated signal is proportional to the population of one- and two-exciton manifolds at $t_4 = 0$, which in turn depend on the delay times t_1, t_2, and t_3 and the phases of the pulses. By selecting a certain phase combination, e.g., rephasing, nonrephasing, or double-quantum coherence, and assuming that all chromophores have identical quantum yield Φ, the time-integrated signal can be written as

$$\bar{S} = \Phi \sum_{n=1} P_{e_n g}(0) + (2-\alpha)\Phi \sum_{n=1} \sum_{m>n} P_{e_n e_m}(0) \tag{10}$$

https://doi.org/10.1021/acs.jpclett.3c02824
J. Phys. Chem. Lett. 2023, 14, 11438−11446

where the parameter α quantifies the deviation of the contribution of the two-exciton manifold from twice that of the one-exciton manifold. In the Supporting Information, we derive eq 10 from a kinetic model for the populations during the detection time, including exciton recombination, EEA, and different signal generation rates of the one- and two-exciton manifolds.

The different pathways that generate populations on the one- and two-exciton manifold upon light−matter interaction can be visualized in terms of Feynman diagrams (FDs). In Figure 3a, we report FDs for the rephasing signal considering the ground state $|0\rangle$, the one-exciton state $|1\rangle$, and the two-exciton state $|2\rangle$. Notice that pathways that are in a coherence during the waiting time t_2 have been neglected. In the weak coupling limit, this coherence is established between (localized) site states rather than (delocalized) excitonic states. Because this coherence dephases at twice the rate of the optical coherence, these pathways can be neglected when the dephasing time is comparable to the pulse duration.

The pathways are distinguished into ground-state bleaching (GSB), stimulated emission (SE), and excited-state absorption (ESA) processes. While both GSB and SE pathways end in a one-exciton population, the presence of a fourth pulse gives rise to two kinds of ESA pathways, ending either in a one-exciton (ESAI) or in a two-exciton (ESAII) population. Each pathway contributes to the signal with a sign $(-1)^{n_B}$, where n_B is the number of interactions on the *bra* side of the FD. Therefore, GSB, SE, and ESAI contribute with negative features to the spectrum, while ESAII comes with positive sign. Depending on their sign, spectral features associated with different pathways may interfere constructively or destructively within the spectrum, eventually leading to partial or complete cancellation.

In weakly interacting systems, FDs can be differentiated into self- and cross-population pathways,[25] respectively identified by the superscript "s" and "c" in Figure 3a. In self-population pathways, the four pulses interact with the same chromophore, while in cross-population pathways, each pair of pulses interacts with different chromophores. Because self- and cross-population pathways have the same phase relation, they are extracted together in the signal. To comprehend their contribution to the final spectrum, we need to understand how the different pathways combine in the signal. Notice that in the present model, ESA-type contributions are all cross-population pathways simply because we have assumed that each molecule is described as a two-level system. While this assumption simplifies the analysis of the signal, it can be relaxed by including the double excited state of each molecule.

First, consider the ideal case where the two-exciton state contributes twice as much as the one-exciton state to the signal, corresponding to $\alpha = 0$ in eq 10. This is realized in the absence of EEA and when the signal generation rate of the two-exciton manifold is twice that of the one-exciton manifold. Under these conditions, the signal reduces to the sum of the nonlinear response of independent chromophores, that is

$$\overline{S} = \Phi \sum_{n=1} P_{e_n}(0) \tag{11}$$

where the single chromophore population results from the sum over that of the collective states, $P_{e_n} = P_{e_n g} + \sum_{m\neq n} P_{e_n e_m}$. In this case, only the GSB and SE self-population pathways contribute to the spectrum, meaning that the ESAII cross-population pathways exactly cancel the GSB and ESAI cross-population pathways. This corresponds to the situation with $N = 1$ in eqs 6 and 7, recovering an equal intensity of GSB and SE contributions to the nonlinear signal while other sources of nonlinearity are absent.

The situation changes when $\alpha > 0$. Let us consider the case where the assembly of N molecules generates the same signal independently of the number of excitations so that the one- and two-exciton manifolds contribute equally, corresponding to $\alpha = 1$ in eq 10. In the Supporting Information, we show that this situation can result either because of fast EEA during t_4 or when the two-exciton manifold generates the signal at the same rate as the one-exciton manifold, in the absence of EEA. In this case, which identifies the limit of complete annihilation, the signal can be written as

$$\overline{S} = \Phi \sum_{n=1} P_{e_n g}(0) + \Phi \sum_{n=1} \sum_{m>n} P_{e_n e_m}(0) = \Phi \sum_{n=1} P_{e_n}(0) - \Phi \sum_{n=1} \sum_{m>n} P_{e_n}(0) \times P_{e_m}(0) \tag{12}$$

Notice that the contribution of the two-exciton state to the signal is reduced, resulting in mutual cancellation between the ESAII and ESAI cross-population pathways. Therefore, in addition to the self-population pathways from GSB and SE, the GSB cross-population pathways also contribute to the spectrum. This contribution to the signal corresponds to the nonlinearity due to the reduced response of the assembly, resulting from eqs 6 and 7 for $N > 1$.

The second equality in eq 12 shows that in the case of weak coupling between different chromophores, the population of the two-exciton manifold at $t_4 = 0$ can be factorized as $P_{e_n e_m}(0) = P_{e_n}(0) \times P_{e_m}(0)$. Therefore, the additional signal boils down to the product of the linear signals of the individual molecules. This is analogous to the phenomenon of incoherent mixing[22,24,25] as we will further discuss below.

A key point to note is the different scaling of the number of self- and cross-population pathways: GSB involves N self-population pathways and $N(N-1)$ cross-population pathways, while SE involves N self-population pathways (Figure 3b). This is reflected in the number of linear and product terms contributing to the signal in eq 12. As N increases, the striking consequence in the spectrum is the dominance of GSB cross-population contributions over the self-population signal, in analogy with the ratio resulting from the probabilistic analysis in eq 9. Indeed, the ratio between the number of SE and GSB pathways is

$$\frac{\mathrm{SE}}{\mathrm{GSB}} = \frac{\mathrm{SE}^s}{\mathrm{GSB}^s + \mathrm{GSB}^c} = \frac{N}{N + N(N-1)} = \frac{1}{N} \tag{13}$$

resulting that, for large N, the GSB contribution can completely dominate over the SE contribution, in the limiting case of $\alpha = 1$. Furthermore, we also notice that the ratio between the number of self- and cross-population pathways is

$$\frac{\mathrm{self}}{\mathrm{cross}} = \frac{\mathrm{GSB}^s + \mathrm{SE}^s}{\mathrm{GSB}^c} = \frac{2N}{N(N-1)} = \frac{2}{N-1} \tag{14}$$

meaning that for large N, the nonlinear signal is dominated by cross-population pathways.

These ratios are important to assess the information content in the spectra as SE is the only pathway containing information about the excited-state dynamics along t_2 and self-population

https://doi.org/10.1021/acs.jpclett.3c02824
J. Phys. Chem. Lett. 2023, 14, 11438−11446

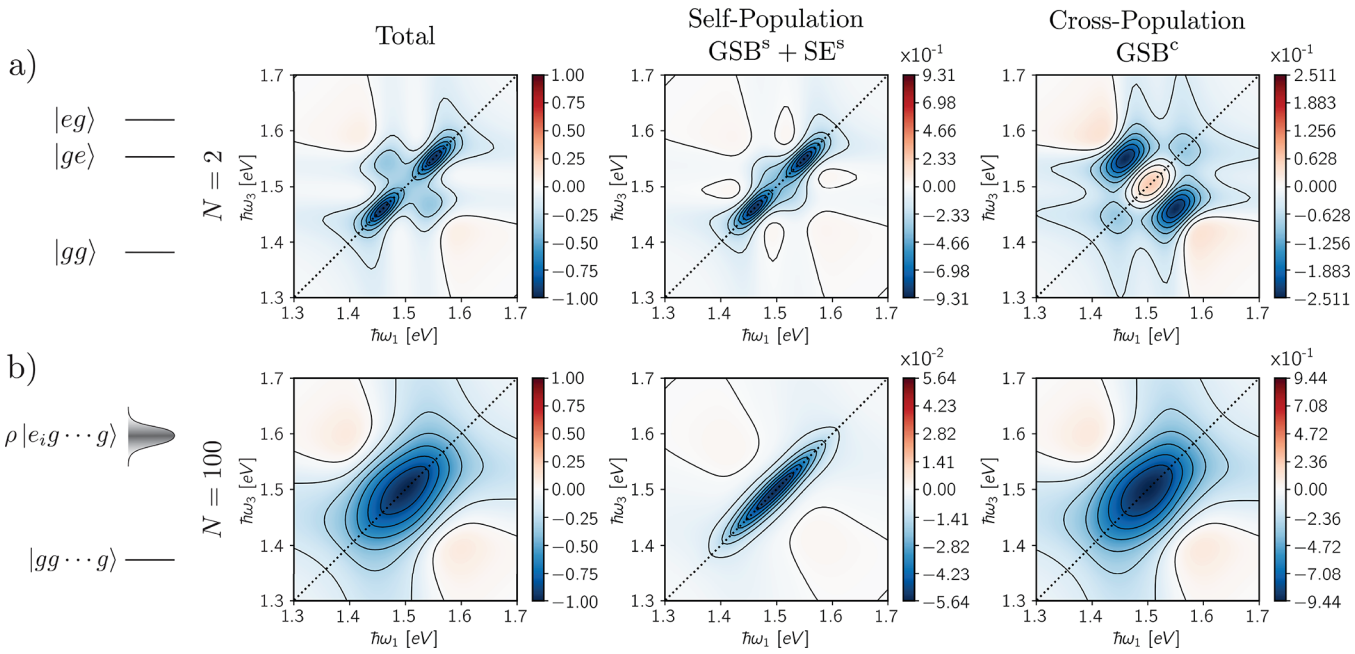

Figure 4. Total (first column), self-population contribution (second column), and cross-population contribution (third column) for the rephasing signal of two different assemblies with (a) $N = 2$ and (b) $N = 100$. On the left, a schematic representation of the energy levels for the two systems.

pathways contain the nonlinear response of the chromophores. As N increases, the contribution of cross-population pathways becomes more significant, reducing the amount of dynamical information. In other words, both self- and cross-population pathways contribute to the spectra, but only the former actually provides information about the excited-state dynamics in the system, while the latter simply reduces to the product of linear responses of the two molecules with no evolution along t_2.

We now consider the interplay between self- and cross-population pathways to the A-2DES spectra at waiting time $t_2 = 0$ fs by varying the number of chromophores N. Assuming $\Phi = 1$ and $\alpha = 1$, in Figure 4 we report the rephasing spectra for $N = 2$ (Figure 4a) and $N = 100$ (Figure 4b), along with the isolated contributions from self- and cross-population pathways. For $N = 2$, we consider two chromophores with different excitation energies so that the net effect is the appearance of well-defined cross-peaks. The transition energies of the two molecules are respectively $\epsilon_1 = 1.55$ eV and $\epsilon_2 = 1.46$ eV. Instead, the energies of the chromophores for $N = 100$ are drawn from a Gaussian distribution with mean $\mu = 1.5$ eV and standard deviation $\sigma = 45$ meV. In both cases, we consider a Voigt line shape function $g(t) = \Gamma t + \Delta^2 t^2$, which accounts for inhomogeneous ($\Delta = 20$ meV) and homogeneous ($\Gamma = 20$ meV) broadenings.

In the case of $N = 2$, the spectrum exhibits two diagonal peaks and two cross-peaks, corresponding to the self- and cross-population contributions, respectively. In this case, the amount of signal associated with cross-population pathways is smaller than the self-population ones, meaning that the dynamical information from the SE contribution is not hidden. On the contrary, for $N = 100$, the spectrum is dominated by a single broad peak mainly due to the contribution of cross-population pathways. By recalling that cross-population contributions in the weak coupling limit reduce to the product of linear signals (incoherent mixing), we suggest that such mixing can happen even in the absence of direct interaction between excitons. Indeed, the emergence of the GSB cross-population contribution is related to the reduced signal generated by the two-exciton manifold, as resulting from eqs 10 and 12. This is reduced because of dynamical processes, e.g., EEA, but also for other intrinsic mechanisms limiting the emission to a single output. In this sense, the case of the reaction center generating charges on a time scale slower than the exciton lifetime is paradigmatic because $\alpha = 1$ even when two independent excitations are generated. Therefore, the emergence of cross-peaks does not necessarily reflect the presence of coupling between molecules or the annihilation between different excitations.

The spectra in Figure 4 refer to $t_2 = 0$. Because we are looking at the rephasing signal, self-population pathways are diagonally elongated whereas cross-population pathways result in inhomogeneously broadened spectra. The different line shape reflects the fact that fluctuations on the same molecule are correlated, while those on different molecules are uncorrelated.[36] A discussion about the line shape of self- and cross-population pathways in the presence of homogeneous and inhomogeneous broadenings is reported in the Supporting Information. The evolution of the spectral line shape for longer t_2 is not considered explicitly here; however, while the line shape of the self-population pathways reflects the evolution of the wavepacket during t_2, the GSB cross-population pathway only reflects the recovery of the ground state as much as the overall nonlinear signal. Moreover, as t_2 increases, energy transfer between different molecules can take place, resulting in cross-peaks carrying information about the excited-state dynamics. However, because these pathways would have the same weight as the self-population pathways from which they originate, we also expect them to be hidden by cross-population pathways when N is large.

In summary, we considered the different sources of nonlinearity in the response of a molecular assembly excited by multiple pulses in the case of action detection. The probabilistic analysis offers a practical interpretation of the

https://doi.org/10.1021/acs.jpclett.3c02824
J. Phys. Chem. Lett. 2023, 14, 11438−11446

signal contributions described by the response theory. For example, cancellation of the ESA pathways in the fourth-order response simply corresponds to the fact that when only one excitation can be detected, the number of excitation events does not change the output.

Therefore, we can conclude that when the output is not proportional to the number of excited molecules, action-detected spectroscopy cannot isolate pathways in which the interaction occurs on the same molecule (self-population pathways) or on different molecules (cross-population pathways). In the worst-case scenario of complete annihilation, i.e., $\alpha = 1$, the ratio between self- and cross-population pathways is $2/(N - 1)$, where only the former brings dynamical information. Moreover, we highlight that the excited-state dynamics along t_2 is exclusively present in the SE contribution. Because the ratio SE/GSB has $1/N$ as an upper limit, the SE contribution is likely to be hidden or negligible for large N.

As a result, we are able to identify the origin of incoherent mixing as due to the fourth-order terms that correspond to GSB cross-population pathways, where the two coherences along t_1 and t_3 occur on different molecules but result in a single output. In a 2D spectrum of a weakly interacting assembly, GSB cross-population pathways correspond to the product of the two linear signals and do not show evolution along t_2 beyond ground-state recovery. Thus, for large N, A-2DES measurements would likely provide information equivalent to that of linear absorption. We can apply this argument to different systems as the key factor is the ratio between the number of output and excitation sites, which is $1/N$ in the case of equal contributions of the one- and two-exciton manifolds in the weak coupling scenario.

We report that excitonic coupling may change the result and play a positive role. Indeed, while the contribution of the two-exciton manifold can still be suppressed by efficient EEA or nonlinear signal generation mechanisms, the number of optically active GSB cross-population contributions may be reduced because of dipole moment redistribution. In this more general setting, N should be identified with the number of absorbing states rather than the number of independent chromophores. Moreover, in the case of strong excitonic coupling, cross-population pathways reflect the presence of delocalization in the system.[16,37]

An unexpected mitigation of the unfavorable scaling of self-population pathways comes from disorder. Indeed, the presence of inhomogeneous broadening improves the visibility of self-population pathways compared with cross-population pathways. This aspect is linked to the rephasing capability of the nonlinear response, as shown explicitly in the Supporting Information.

When it is known that the signal corresponds to the case of complete annihilation ($\alpha = 1$), a potential advantage comes from the possibility of estimating N itself. N could be an indicator of how many chromophores are connected to the output, such as the number of chlorophylls linked to the reaction center in a photosynthetic system. The estimation of N would become feasible if SE and GSB could be measured independently. For example, it is possible to design an experiment where the pump pulse overlaps only with the lower energies of the absorption band and the probe with the full band. Close to $t_2 = 0$, the A-2DES signal will exhibit both SE and GSB components at the pump frequencies, whereas only the GSB component will be present at higher frequencies, where the probe does not overlap with the pump.

Nevertheless, action spectroscopy has strong limits in its use on a wide range of materials. For this reason, it is then crucial to be aware of the kind of samples to be studied with action-detected spectroscopies. Grégoire et al. showed that incoherent mixing can contribute differently depending on the amount of EEA in the sample.[22] Indeed, it has been found that incoherent mixing does not contribute significantly to the A-2DES spectrum of organic solar cells, while it dominates over the nonlinear response in perovskite samples. Additionally, cross-peak dynamics has been observed in heterojunction photovoltaic cells.[8] This is possible because a working cell tries to achieve high internal quantum efficiency, implying that from every exciton a charge is produced, meaning a detection for every absorption ($\alpha = 0$ or $N = 1$).

The results reported in this work highlight the importance of strategies to minimize the incoherent mixing contributions to A-2DES. Recently, 2D-FLEX has been proposed, which can selectively measure the SE pathway in fluorescence-detected experiments.[38] Furthermore, the possibility of time-gating the fluorescence signal during the detection time can help to reduce the extent of incoherent mixing.[18−20] However, a time-gating approach is far-fetched to be applied in photocurrent detection.

In this work, we provide a different perspective to the problem of incoherent mixing in action-detected spectroscopy. Our argument refers to an assembly of weakly coupled molecules, and it does not explicitly account for the presence of vibrational degrees of freedom. Future work is needed to understand how strong excitonic coupling may change the relative weight of the different contributions to the signal and to further elucidate the dynamics along the waiting time t_2. On the other hand, the inclusion of higher excited states $|f\rangle$ of each molecule introduces ESA self-population pathways providing additional spectral features, without affecting the scaling between SE and GSB contributions. A further step will be to consider higher-order response in the light−matter interaction in order to investigate the signal coming from multiexciton states.[39,40]

■ ASSOCIATED CONTENT

Supporting Information

The Supporting Information is available free of charge at https://pubs.acs.org/doi/10.1021/acs.jpclett.3c02824.

Derivation of the time-integrated signal from a kinetic model for population, details of response function and line shape used for the 2D spectra simulations (PDF)

■ AUTHOR INFORMATION

Corresponding Author

Niek F. van Hulst − *ICFO - Institut de Ciencies Fotoniques, The Barcelona Institute of Science and Technology, Barcelona 08860, Spain; ICREA - Institució Catalana de Recerca i Estudis Avançats, Barcelona 08010, Spain;* orcid.org/0000-0003-4630-1776; Email: niek.vanhulst@icfo.eu

Authors

Luca Bolzonello − *ICFO - Institut de Ciencies Fotoniques, The Barcelona Institute of Science and Technology, Barcelona 08860, Spain;* orcid.org/0000-0003-0893-5743

Matteo Bruschi − *Department of Chemical Science, University of Padova, Padova 35131, Italy;* orcid.org/0000-0001-7838-0363

https://doi.org/10.1021/acs.jpclett.3c02824
J. Phys. Chem. Lett. 2023, 14, 11438−11446

Barbara Fresch − *Department of Chemical Science, University of Padova, Padova 35131, Italy; Padua Quantum Technologies Research Center, Università degli Studi di Padova, Padova 35122, Italy;* orcid.org/0000-0002-0988-0644

Complete contact information is available at: https://pubs.acs.org/10.1021/acs.jpclett.3c02824

Author Contributions

L.B. and M.B. contributed equally to this work.

Notes

The authors declare no competing financial interest.

■ ACKNOWLEDGMENTS

The authors thank Dr. Manuel López-Ortiz and Dr. Pau Gorostiza Langa for fruitful discussions. N.F.v.H. acknowledges the financial support through the MCIN/AEI projects PID2021-123814OB-I00, TED2021-129241B-I00, the "Severo Ochoa" program for Centres of Excellence in R&D CEX2019-000910-S, Fundacio Privada Cellex, Fundacio Privada Mir-Puig, the Generalitat de Catalunya through the CERCA program, the European Commission (ERC Advanced Grant 101054846 - FastTrack), and QuantERA project no. 731473 and 101017733: ExTRaQT. L.B. received funding from the Clean Planet Program supported by Fundacio Joan Ribas Araquistain (FJRA). M.B. and B.F. acknowledge the financial support by the Department of Chemical Sciences (DiSC) and the University of Padova with Project QA-CHEM (P-DiSC No. 04BIRD2021-UNIPD).

■ REFERENCES

(1) Collini, E. 2D electronic spectroscopic techniques for quantum technology Applications. *J. Phys. Chem. C* **2021**, *125*, 13096−13108.
(2) Biswas, S.; Kim, J.; Zhang, X.; Scholes, G. D. Coherent two-dimensional and broadband electronic spectroscopies. *Chem. Rev.* **2022**, *122*, 4257−4321.
(3) Tiwari, V. Multidimensional electronic spectroscopy in high-definition - Combining spectral, temporal, and spatial resolutions. *J. Chem. Phys.* **2021**, *154*, 230901.
(4) Karki, K. J.; Ciappina, M. F. Advances in nonlinear spectroscopy using phase modulated light fields: prospective applications in perturbative and non-perturbative regimes. *Adv. Phys.: X* **2022**, *7*, 2090856.
(5) Karki, K. J.; Chen, J.; Sakurai, A.; Shi, Q.; Gardiner, A. T.; Kühn, O.; Cogdell, R. J.; Pullerits, T. Before Förster. Initial excitation in photosynthetic light harvesting. *Chem. Sci.* **2019**, *10*, 7923−7928.
(6) Bakulin, A. A.; Rao, A.; Pavelyev, V. G.; van Loosdrecht, P. H. M.; Pshenichnikov, M. S.; Niedzialek, D.; Cornil, J.; Beljonne, D.; Friend, R. H. The Role of Driving Energy and Delocalized States for Charge Separation in Organic Semiconductors. *Science* **2012**, *335*, 1340−1344.
(7) Karki, K. J.; Widom, J. R.; Seibt, J.; Moody, I.; Lonergan, M. C.; Pullerits, T.; Marcus, A. H. Coherent two-dimensional photocurrent spectroscopy in a PbS quantum dot photocell. *Nat. Commun.* **2014**, *5*, 5869.
(8) Bolzonello, L.; Bernal-Texca, F.; Gerling, L. G.; Ockova, J.; Collini, E.; Martorell, J.; van Hulst, N. F. Photocurrent-Detected 2D Electronic Spectroscopy Reveals Ultrafast Hole Transfer in Operating PM6/Y6 Organic Solar Cells. *J. Phys. Chem. Lett.* **2021**, *12*, 3983−3988.
(9) Roeding, S.; Brixner, T. Coherent two-dimensional electronic mass spectrometry. *Nat. Commun.* **2018**, *9*, 2519.
(10) Aeschlimann, M.; Brixner, T.; Fischer, A.; Kramer, C.; Melchior, P.; Pfeiffer, W.; Schneider, C.; Strüber, C.; Tuchscherer, P.; Voronine, D. V. Coherent Two-Dimensional Nanoscopy. *Science* **2011**, *333*, 1723−1726.
(11) Uhl, D.; Bangert, U.; Bruder, L.; Stienkemeier, F. Coherent optical 2D photoelectron spectroscopy. *Optica* **2021**, *8*, 1316.
(12) Bakulin, A. A.; Silva, C.; Vella, E. Ultrafast Spectroscopy with Photocurrent Detection: Watching Excitonic Optoelectronic Systems at Work. *J. Phys. Chem. Lett.* **2016**, *7*, 250−258.
(13) Tiwari, V.; Matutes, Y. A.; Gardiner, A. T.; Jansen, T. L.; Cogdell, R. J.; Ogilvie, J. P. Spatially-resolved fluorescence-detected two-dimensional electronic spectroscopy probes varying excitonic structure in photosynthetic bacteria. *Nat. Commun.* **2018**, *9*, 4219.
(14) Fersch, D.; Malý, P.; Rühe, J.; Lisinetskii, V.; Hensen, M.; Würthner, F.; Brixner, T. Single-Molecule Ultrafast Fluorescence-Detected Pump−Probe Microscopy. *J. Phys. Chem. Lett.* **2023**, *14*, 4923−4932.
(15) Mueller, S.; Draeger, S.; Ma, X.; Hensen, M.; Kenneweg, T.; Pfeiffer, W.; Brixner, T. Fluorescence-Detected Two-Quantum and One-Quantum−Two-Quantum 2D Electronic Spectroscopy. *J. Phys. Chem. Lett.* **2018**, *9*, 1964−1969.
(16) Malý, P.; Lüttig, J.; Mueller, S.; Schreck, M. H.; Lambert, C.; Brixner, T. Coherently and fluorescence-detected two-dimensional electronic spectroscopy: direct comparison on squaraine dimers. *Phys. Chem. Chem. Phys.* **2020**, *22*, 21222−21237.
(17) Mueller, S.; Lüttig, J.; Brenneis, L.; Oron, D.; Brixner, T. Observing Multiexciton Correlations in Colloidal Semiconductor Quantum Dots via Multiple-Quantum Two-Dimensional Fluorescence Spectroscopy. *ACS Nano* **2021**, *15*, 4647−4657.
(18) Bruschi, M.; Gallina, F.; Fresch, B. Simulating action-2D electronic spectroscopy of quantum dots: insights on the exciton and biexciton interplay from detection-mode and time-gating. *Phys. Chem. Chem. Phys.* **2022**, *24*, 27645−27659.
(19) Malý, P.; Mančal, T. Signatures of Exciton Delocalization and Exciton−Exciton Annihilation in Fluorescence-Detected Two-Dimensional Coherent Spectroscopy. *J. Phys. Chem. Lett.* **2018**, *9*, 5654−5659.
(20) Kunsel, T.; Tiwari, V.; Matutes, Y. A.; Gardiner, A. T.; Cogdell, R. J.; Ogilvie, J. P.; Jansen, T. L. C. Simulating Fluorescence-Detected Two-Dimensional Electronic Spectroscopy of Multichromophoric Systems. *J. Phys. Chem. B* **2019**, *123*, 394−406.
(21) Kühn, O.; Mančal, T.; Pullerits, T. Interpreting Fluorescence Detected Two-Dimensional Electronic Spectroscopy. *J. Phys. Chem. Lett.* **2020**, *11*, 838−842.
(22) Grégoire, P.; Srimath Kandada, A. R.; Vella, E.; Tao, C.; Leonelli, R.; Silva, C. Incoherent population mixing contributions to phase-modulation two-dimensional coherent excitation spectra. *J. Chem. Phys.* **2017**, *147*, 114201.
(23) Bargigia, I.; Gutiérrez-Meza, E.; Valverde-Chávez, D. A.; Marques, S. R.; Srimath Kandada, A. R.; Silva, C. Identifying incoherent mixing effects in the coherent two-dimensional photocurrent excitation spectra of semiconductors. *J. Chem. Phys.* **2022**, *157*, 204202.
(24) Kalaee, A. A. S.; Damtie, F.; Karki, K. J. Differentiation of True Nonlinear and Incoherent Mixing of Linear Signals in Action-Detected 2D Spectroscopy. *J. Phys. Chem. A* **2019**, *123*, 4119−4124.
(25) Bruschi, M.; Bolzonello, L.; Gallina, F.; Fresch, B. Unifying Nonlinear Response and Incoherent Mixing in Action-2D Electronic Spectroscopy. *J. Phys. Chem. Lett.* **2023**, *14*, 6872−6879.
(26) Croce, R.; van Amerongen, H. Light-harvesting in photosystem I. *Photosynth. Res.* **2013**, *116*, 153−166.
(27) Mukamel, S. *Principles of Nonlinear Optical Spectroscopy*; Oxford University Press: 1995.
(28) Mukamel, S. Communication: The origin of many-particle signals in nonlinear optical spectroscopy of non-interacting particles. *J. Chem. Phys.* **2016**, *145*, 041102.
(29) Zhou, N.; Ouyang, Z.; Hu, J.; Williams, O. F.; Yan, L.; You, W.; Moran, A. M. Distinguishing Energy- and Charge-Transfer Processes in Layered Perovskite Quantum Wells with Two-Dimensional Action Spectroscopies. *J. Phys. Chem. Lett.* **2020**, *11*, 4570−4577.

(30) Ouyang, Z.; Zhou, N.; McNamee, M. G.; Yan, L.; Williams, O. F.; You, W.; Moran, A. M. Multidimensional time-of-flight spectroscopy. *J. Chem. Phys.* **2021**, *154*, 220901.
(31) McNamee, M. G.; Ouyang, Z.; Yan, L.; Gan, Z.; Zhou, N.; Williams, O. F.; You, W.; Moran, A. M. Uncovering Transport Mechanisms in Perovskite Materials and Devices with Recombination-Induced Action Spectroscopies. *J. Phys. Chem. C* **2023**, *127*, 2782−2791.
(32) Rojas-Gatjens, E.; Yallum, K. M.; Shi, Y.; Zheng, Y.; Bills, T.; Perini, C. A. R.; Correa-Baena, J.-P.; Ginger, D. S.; Banerji, N.; Silva-Acuña, C. Resolving Nonlinear Recombination Dynamics in Semiconductors via Ultrafast Excitation Correlation Spectroscopy: Photoluminescence versus Photocurrent Detection. *J. Phys. Chem. C* **2023**, *127*, 15969−15977.
(33) Tian, P.; Keusters, D.; Suzaki, Y.; Warren, W. S. Femtosecond Phase-Coherent Two-Dimensional Spectroscopy. *Science* **2003**, *300*, 1553−1555.
(34) Tan, H.-S. Theory and phase-cycling scheme selection principles of collinear phase coherent multi-dimensional optical spectroscopy. *J. Chem. Phys.* **2008**, *129*, 124501.
(35) Tekavec, P. F.; Lott, G. A.; Marcus, A. H. Fluorescence-detected two-dimensional electronic coherence spectroscopy by acousto-optic phase modulation. *J. Chem. Phys.* **2007**, *127*, 214307.
(36) Yang, M.; Fleming, G. R. Third-order nonlinear optical response of energy transfer systems. *J. Chem. Phys.* **1999**, *111*, 27−39.
(37) Schröter, M.; Pullerits, T.; Kühn, O. Using fluorescence detected two-dimensional spectroscopy to investigate initial exciton delocalization between coupled chromophores. *J. Chem. Phys.* **2018**, *149*, 114107.
(38) Yang, J.; Gelin, M. F.; Chen, L.; Šanda, F.; Thyrhaug, E.; Hauer, J. Two-dimensional fluorescence excitation spectroscopy: A novel technique for monitoring excited-state photophysics of molecular species with high time and frequency resolution. *J. Chem. Phys.* **2023**, *159*, 074201.
(39) Malý, P.; Lüttig, J.; Rose, P. A.; Turkin, A.; Lambert, C.; Krich, J. J.; Brixner, T. Separating single- from multi-particle dynamics in nonlinear spectroscopy. *Nature* **2023**, *616*, 280.
(40) Lüttig, J.; Rose, P. A.; Malý, P.; Turkin, A.; Bühler, M.; Lambert, C.; Krich, J. J.; Brixner, T. High-order pump−probe and high-order two-dimensional electronic spectroscopy on the example of squaraine oligomers. *J. Chem. Phys.* **2023**, *158*, 234201.

https://doi.org/10.1021/acs.jpclett.3c02824
J. Phys. Chem. Lett. 2023, 14, 11438−11446